Table 3.1

i	l_i (m)	D_i (m)	λ_i	R_i
1	600	0.4	0.02	96.83
2	600	0.4	0.02	96.83
3	300	0.3	0.03	306.00
4	300	0.3	0.03	306.00
5	300	0.3	0.03	306.00
6	300	0.2	0.04	3098.00
7	300	0.2	0.04	3098.00
8	300	0.2	0.04	3098.00
9	300	0.3	0.03	306.00
10	600	0.3	0.03	612.00
11	300	0.3	0.03	306.00
12	900	0.2	0.04	9295.5
13	300	0.2	0.04	3098.00

Table 3.2

	1	2	3	4	5	6	7	8	9	10	11	12	$13=i_{max}$
1	−1	+1	0	0	+1	0	0	+1	0	−1	0	0	0
2	0	0	+1	+1	−1	−1	0	0	0	0	0	0	0
3	0	0	0	0	0	+1	+1	−1	−1	0	0	0	0
4	0	0	0	0	0	0	0	0	+1	+1	−1	−1	−1

satisfy the continuity conditions at the nodes. The signs are given according to the positive direction around each mesh (Table 3.2).

(3) The branch–node matrix is formed.

(4) The solution by the Hardy-Cross method is programmed.

```
C     H.CROSS SOLUTION OF PIPE NETWORK
      DIMENSION R(40),Q(40),M(40,40),U(40),DH(40)
     1D(40)
      READ(5,1) TEST,IMAX,KMAX
    1 FORMAT(F7.0,2I4)
      READ(5,10)(Q(I),I=1,IMAX)
      READ(5,10)(D(I),I=1,IMAX)
      DO 11 K=1,KMAX
   11 READ(5,12)(M(K,I),I=1,IMAX)
      READ(5,10)(R(I),I=1,IMAX)
   12 FORMAT(13I4)
   10 FORMAT(10F7.0)
      ITER=0
   40 ITER=ITER+1
      IF (ITER.GT.500) STOP 1
      DIFMX=0.
      DO 20 K=1, KMAX
      SUM1=0.
      SUM2=0.
      DO 25 I=1, IMAX
      T=M(K,I)
      SUM1=SUM1+T*R(I)*Q(I)**2
   25 SUM2=SUM2+2.*ABS(T)*Q(I)*R(I)
      DQ=-SUM1/SUM2
      IF(ABS(DQ).GT.DIFMX) DIFMX=ABS(DQ)
      DO 30 I=1, IMAX
      Q(I)=Q(I)+M(K,I)*DQ
      IF(Q(I).GT.0.) GO TO 30
      Q(I)=-Q(I)
      DO 35 KK=1, KMAX
   30 CONTINUE
   20 CONTINUE
      IF(DIFMX.GT.TEST) GO TO 40
      DO 70 I=1, IMAX
      U(I)=Q(I)*1.273/D(I)**2
   70 DH(I)=R(I)*Q(I)**2
      WRITE(6,75) ITER
   75 FORMAT(//I8//)
      WRITE(6,45)(Q(I), I=1, IMAX)
      WRITE(6,45)(U(I), I=1, IMAX)
      WRITE(6,45)(DH(I), I=1, IMAX)
      DO 65 K=1,KMAX
   65 WRITE(6,55)(M(K,I),I=1, IMAX)
   45 FORMAT(10F10.4)
   55 FORMAT(10I6)
      STOP
      END
```


The final discharge values along the branches (for a convergence criterion TEST = 0.1) and the calculated pressure heads at the nodes are depicted in Fig. 3.4.

3.3. NON-STEADY FLOW. WATER HAMMER

Unsteady flow in closed conduits becomes very important in the case of sudden changes of discharge due to the interruption of a pump operation, or the closing or opening of a vane. These variations create pressure waves propagating with alternating sign (high pressure or low pressure) along a pipe. The computational goal is usually to find the extreme pressure values in order to check the safety of the conduit.

Assuming elastic conduit walls and compressible fluid the velocity of an elastic wave along the pipe is found to be

$$c=\sqrt{\left\{\frac{1}{\rho\left(\frac{1}{K}+\frac{D}{Ee}\right)}\right\}} \tag{3.16}$$

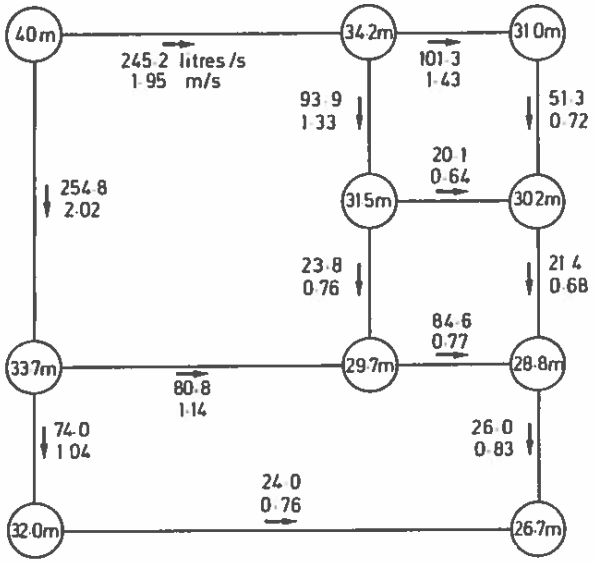

Fig. 3.4

where ρ is the water density, K the water modulus of elasticity ($K = 2 \times 10^8\ k\rho/m^2$), D the pipe diameter, e the walls thickness, and E the modulus of elasticity of the pipe material ($E = 2 \times 10^{10}\ K\rho/m^2$ for steel pipes).

Approximating the pipe body by a series of rings (negligible Poisson ratio) with uniform internal pressure, we can correlate the relative pressure inside the pipe to the pipe diameter,

$$H = \frac{2c^2}{g}\frac{r - r_0}{r} \tag{3.17}$$

where r is the radius under pressure head H and r_0 the radius under pressure head equal to zero (absolute pressure = 1 atm).

The mathematical model is formed using the quantitative expression for the principle of mass continuity and force equilibrium, written with respecto the unknown functions H, V (pressure head and water velocity) as:

$$\frac{\partial V}{\partial t} + V\frac{\partial V}{\partial x} + g\frac{\partial H}{\partial x} = -\frac{2\tau_0}{r} \tag{3.18}$$

$$\frac{\partial H}{\partial t} + V\frac{\partial H}{\partial x} + \frac{c^2}{g}\frac{\partial V}{\partial x} = 0 \tag{3.19}$$

where τ_0 is the wall shear stress, which can be expressed as

$$\tau_0 = KV|V| \tag{3.20}$$

where

$$K = \lambda\rho/8 \tag{3.21}$$

a friction coefficient depending on the pipe diameter and roughness.

During the numerical integration of Equations 3.18 and 3.19 using finite difference methods, some difficulties arise on the upstream and downstream boundaries where the H, V values, on and outside these boundaries are needed. This difficulty can be overcome using the properties of the corresponding characteristic curves. A considerable simplification is achieved by neglecting the non-linear terms $V\partial V/\partial x$ and $V\partial H/\partial x$.

As the frictional losses are usually small, due to the short duration of the phenomenon and the moderate velocity values, the system of Equations 3.18 and 3.19 can be simplified to the final form,

$$\frac{\partial V}{\partial t} + g\frac{\partial H}{\partial x} = 0 \tag{3.22}$$

$$\frac{\partial H}{\partial t} + \frac{c^2}{g}\frac{\partial V}{\partial x} = 0 \tag{3.23}$$

The model is completed by the initial and boundary conditions.

The velocity and pressure heads are given before the initiation of the velocity variations. The boundary conditions are usually either of the reservoir type, where the pressure head is constant (equal to the hydrostatic pressure) or of the vane type. In the case of a suddenly closed vane the velocity is zero and in the case of a slowly closing or opening vane the continuity principle leads to the condition,

$$V = \frac{S}{S_0}\sqrt{(2gH)} \tag{3.24}$$

where $S = S(t)$ is the flow section, S_0 the initial vane opening and H the pressure head.

The numerical integration of the system describing the propagation of pressure and discharge waves along the pipe, with or

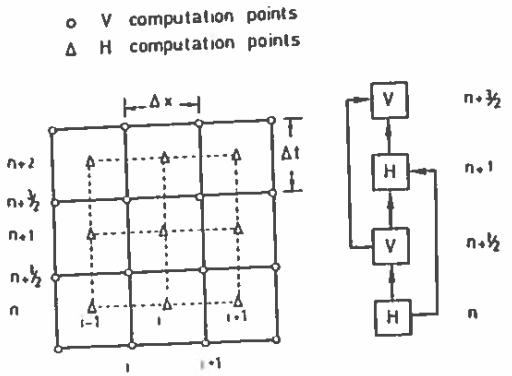

Fig. 3.5

without simultaneous energy dissipation due to friction, can be done by the developed FD schemes.

A simple explicit scheme will be used here directly applied to a staggered grid. The grid is characterised by temporal and spatial eccentricity. The pipe is discretised in characteristic sections. The velocity values are computed for each section while the pressure heads refer to the reaches between two sections. The H and V computations are performed at different time levels. The H^n, H^{n+1} ... and $V^{n+\frac{1}{2}}$, $V^{n+\frac{3}{2}}$ ... values are interchangeably computed. The grid in x–t space and the integration procedure are schematically given in Fig. 3.5. The approximation of Equations 3.22 and 3.23 by difference equations leads to,

$$\frac{V_i^{n+3/2}-V_i^{n+1/2}}{\Delta t}+g\frac{H_i^{n+1}-H_{i-1}^{n+1}}{\Delta x}=0 \tag{3.25}$$

$$\frac{H_i^{n+1}-H_i^n}{\Delta t}+\frac{c^2}{g}\frac{V_{i+1}^{n+1/2}-V_i^{n+1/2}}{\Delta x}=0 \tag{3.26}$$

where i and n are space and time indices respectively.

An application for an isolated pipe starting from a reservoir and terminated by a closing vane is given in the following example. The closing time is smaller than $2L/c$ where L is the pipe length.

EXAMPLE 3.2

To compute the pressure head variations on the downstream end of a pipe $L=6000$ m long with $D=0.5$ m, $e=4$ mm, $H_0=5$ m and $V_0=$

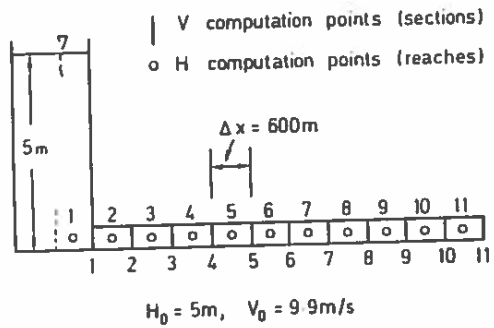

Fig. 3.6

9.9 m/s. The discharge is interrupted through a downstream vane at $t=2$ s with a linear decrease of the flow section. Frictional losses are negligible.

A general plan of the reservoir-pipe system and the pipe discretisation is included in Fig. 3.6. The solution is performed by means of Equations 3.25 and 3.26. At the upstream end the pressure head, equal to the reservoir depth, is constant. At the downstream end the boundary condition relates velocity and flow section. The wave speed is computed from Equation 3.16 and is found to be $c=$ 2980 m/s. The integration time step Δt is taken equal to 0.1 s so that the Courant condition is satisfied.

$$\frac{c\Delta t}{\Delta x}=0.496<1 \tag{3.27}$$

The solution is programmed in FORTRAN as follows:

```
C     WATER HAMMER FINITE DIFF SOLUTION
      DIMENSION V(100), H(100)
      READ(5,1)DX,DT,C,HO,VO,TOL,IMAX
    1 FORMAT(6F7.0,I4)
      IMAX1=IMAX-1
      DO 2 I=1, IMAX
      V(I)=VO
    2 H(I)=HO
      T=0.
      N=0
  100 T=T+DT
      N=N+1
      IF(T.GT.TOL) GO TO 3
      SR=(TOL-T)/TOL
      GO TO 4
```

```
    3   SR=0.
    4   CONTINUE
        V(IMAX)=SR*SQRT(2.*9.81*HO)
        DO 5 I=2,IMAX1
    5   V(I)=V(I)-9.81*DT*(H(I)-H(I-1))/DX
        DO 6 I=2,IMAX1
    6   H(I)=H(I)-DT*C**2/9.81*(V(I+1)-V(I))/DX
        WRITE(6,11) T
   11   FORMAT (//F10.3//)
        WRITE(6,12)(V(I),I=1,IMAX)
        WRITE(6,12)(H(I),I=1,IMAX)
   12   FORMAT(12F10.4)
        IF(N.LT.200) GO TO 100
        STOP
        END
```

For data values DX = 600 m, DT = 0.1 s, HO = 5 m, VO = 9.9 m/s, TOL = 2 s (closure time) and IMAX = 12 sections. The pressure variation at the downstream end is graphically presented in Fig. 3.7.

The accuracy achieved by the numerical solution is satisfactory as the analytical solution gives for the maximum excess pressure

$$\Delta H = \frac{c\Delta V}{g} = 3010 \text{ m} \tag{3.28}$$

a value differing very little from the numerically computed one. The method does not contain any numerical diffusion as the maximum and minimum pressure values are periodically repeated in the absence of frictional losses.

The linearised model, Equations 3.22 and 3.23, applied here presents no difficulty on the boundaries as the non-linear $V\partial V/\partial x$ and $V\partial V/\partial x$ terms are dropped. The inclusion of these terms for rapidly varying velocity fields, as in the case of very deformable pipe walls and in the case of open conduits, would introduce some complications.

The property of characteristics is used here and in Chapter 4 at an introductory level as this facilitates both the understanding of the wave propagation mechanism and the computational procedures.

If Equation 3.23 is multiplied by g/c and successively added and subtracted from Equation 3.22 the following relations result:

$$\frac{\partial}{\partial t}\left(V+\frac{gH}{c}\right)+c\frac{\partial}{\partial x}\left(V+\frac{gH}{c}\right)=0 \tag{3.29}$$

$$\frac{\partial}{\partial t}\left(V-\frac{gH}{c}\right)-c\frac{\partial}{\partial x}\left(V-\frac{gH}{c}\right)=0 \tag{3.30}$$

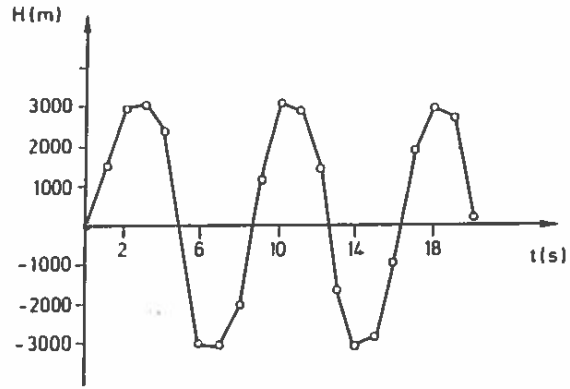

Fig. 3.7

If the dx/dt derivatives are replaced by $+c$ and $-c$ respectively in Equations 3.29 and 3.30 they take the form

$$\frac{d}{dt}\left(V+\frac{gH}{c}\right)=0, \quad \text{along} \quad \frac{dx}{dt}=c \tag{3.31}$$

$$\frac{d}{dt}\left(V-\frac{gH}{c}\right)=0, \quad \text{along} \quad \frac{dx}{dt}=-c \tag{3.32}$$

where d/dt denotes the total or material derivative.

The physical meaning of Equations 3.31 and 3.32 is that the characteristic lines are straight lines of slope $+c$ and $-c$ and the $V\pm(gH/c)$ values are kept constant along those lines. Their numerical integration can be realised on the characteristic lines or, for reasons of easier geometric description of the flow domain, on an orthogonal grid established in the x–t plane. A simple explicit procedure of integration on the orthogonal grid will be presented below.

The notation to be used is presented in Fig. 3.8. The characteristics AL, AR with slopes $+c$ and $-c$, respectively, pass through the point A where the values of V and H are to be computed. If the inequality $\Delta x > c\Delta t$ is satisfied, points L and R lie between points $i-1, i$ and $i, i+1$, respectively. The sums $V+(gH/c)$, $V-(gH/c)$ are known to be constant along these lines.

The values of V, H on L and R (V_L, H_L, V_R, H_R) can be easily computed by means of linear interpolation from the known values $V^n_{i-1}, V^n_i, V^n_{i+1}, H^n_{i-1}, H^n_i, H^n_{i+1}$. On this basis, the following algorithm can be formulated:

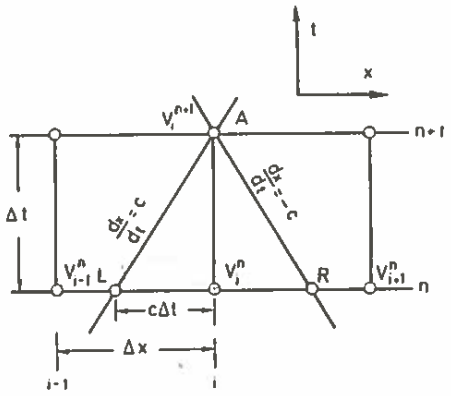

Fig. 3.8

(1) Computation of V_L, H_L, V_R, H_R:

$$V_L = V_i^n + (V_{i-1}^n - V_i^n)c\Delta t/\Delta x \tag{3.33}$$

$$V_R = V_i^n + (V_{i+1}^n - V_i^n)c\Delta t/\Delta x \tag{3.34}$$

$$H_L = H_i^n + (H_{i-1}^n - H_i^n)c\Delta t/\Delta x \tag{3.35}$$

$$H_R = H_i^n + (H_{i+1}^n - H_i^n)c\Delta t/\Delta x \tag{3.36}$$

(2) Computation of the auxiliary quantities AL, AR by means of Equations 3.33–3.36:

$$AL = V_L + \frac{g}{c} H_L \tag{3.37}$$

$$AR = V_R - \frac{g}{c} H_R \tag{3.38}$$

(3) Computation of V_i^{n+1}, H_i^{n+1} from Equations 3.31 and 3.32:

$$V_i^{n+1} = (AL + AR)/2 \tag{3.39}$$

$$H_i^{n+1} = (AL - AR)/(2*c/g) \tag{3.40}$$

The H values are known on the upstream boundary and the V values can be computed from the AR characteristic by means of the relation

$$V_1^{n+1} = \frac{g}{c} H_1^{n+1} + AR_1 \tag{3.41}$$

The velocity values are known on the downstream boundary and the H values can be computed from the AL characteristic

$$H_{imax}^{n+1} = (AL_{imax} - V_{imax}^{n+1})c/9.81 \tag{3.42}$$

The algorithm can be programmed in FORTRAN as follows:

```
C     WATER HAMMER SOLUTION BY CHARACTERISTICS
      DIMENSION AL(40), AR(40), V(40), H(40)
      READ(5,1) DX,DT,C,HO,VO,TOL,IMAX
    1 FORMAT(6F7.0,I4)
      IMAX1=IMAX-1
      DO 2 I=1,IMAX
      V(I)=VO
    2 H(I)=HO
      N=0
      T=0.
  100 T=T+DT
      N=N+1
      DO 3 I=2,IMAX
    3 AL(I)=V(I)+9.81/C*H(I)+(-V(I)-9.81/C*H(I)+
     1  V(I-1)+9.81/C*H(I-1))*C*DT/DX
      DO 5 I=1,IMAX1
    5 AR(I)=V(I)-9.81/C*H(I)+(-V(I)+9.81/C*H(I)+
     1  V(I+1)-9.81/C*H(I+1))*C*DT/DX
      IF (T.GT.TOL) GO TO 33
      SR=(TOL-T)/TOL
      GO TO 34
   33 SR=0.
   34 CONTINUE
      H(IMAX)=(AL(IMAX)-V(IMAX))*C/9.81
      H(1)=HO
      V(1)=9.81/C*H(1)+AR(1)
      V(IMAX)=SR*SQRT(2.*9.81*HO)
      DO 6 I=2,IMAX1
      V(I)=(AL(I)+AR(I))/2.
    6 H(I)=(AL(I)-AR(I))*C/2./9.81
      WRITE(6,10) T
   10 FORMAT(//5X, 'TIME',F10.3//)
      WRITE(6,12)(H(I),I=1,IMAX)
      WRITE(6,12)(V(I),I=1,IMAX)
   12 FORMAT(11F10.4)
      IF (N.LT.200) GO TO 100
      STOP
      END
```

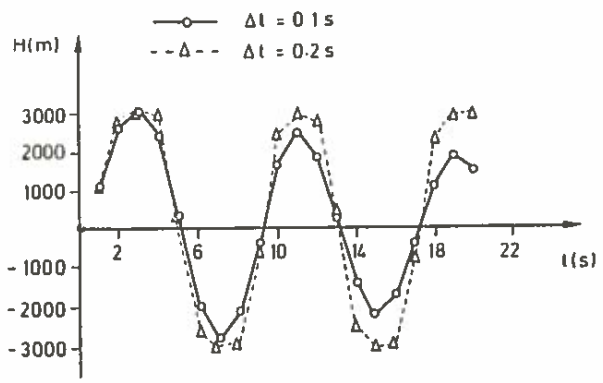

Fig. 3.9

EXAMPLE 3.3

Repeat Example 3.2 using for the numerical integration the properties of characteristics. The pressure variation at the downstream end is to be computed for $t=0.1$ s and $t=0.2$ s.

The application of the above program to the previous data values results in the velocity and pressure head values at the characteristic sections of the pipe. The pressure variation at the downstream end is graphically represented in Fig. 3.9.

It is evident that the explicit scheme using the properties of characteristics contains some inherent numerical dissipation not apparent in the previous solution of Example 3.2. The dissipation seems to vary in inverse proportion to the Δt value. As the value of $c\Delta t/\Delta x$ tends to unity the numerical dissipation decreases. The maximum pressure tends to that found analytically, i.e. 3010 m.

4

Open channel flow

4.1. MATHEMATICAL MODELS FOR NON-STEADY FLOW IN OPEN CHANNELS

Unsteady flow with a free surface forms one of the most interesting areas of hydraulics. Long waves and tidal flow in estuaries, the propagation of floods along natural water-courses, transient flow in irrigation canals due to discharge and level fluctuations are only some examples that fall into this category.

The mathematical model of flow in an open channel with variable cross-section, extending in one dimension in the x direction, contains as unknown functions the mean velocity over a cross section $V=V(x,t)$ and the flow depth $h=h(x,t)$, measured from the lowest part of the cross section to the free surface. It can be synthesized from the quantification of the basic principles of mass continuity and conservation of momentum between two cross-sections. According to the notation of Fig. 4.1 it can take the form

$$B\frac{\partial h}{\partial t}+\frac{\partial}{\partial x}(AV)=0 \tag{4.1}$$

$$\frac{\partial V}{\partial t}+V\frac{\partial V}{\partial x}-g(S_0-S_f)+g\frac{\partial h}{\partial x}=0 \tag{4.2}$$

The slope of the energy line S_f can be approximated, even in the case of unsteady flow, by means of semi-empirical formulae valid for steady flow (the Manning or Chézy equations),

$$S_f=\frac{V^2}{K^2R^{4/3}}=\frac{V^2}{C^2R} \tag{4.3}$$

where K and C are the Manning and Chézy friction coefficients, respectively, and R the hydraulic radius, $R=A/P$. In the case of a channel of large width, B, in comparison to depth, Equation 4.1 can take the form,